Magnetic field of an in-plane vortex outside a layered superconductor

J. R. Kirtley

IBM T.J. Watson Research Center, P.O. Box 218, Yorktown Heights, New York 10598

V. G. Kogan and J. R. Clem

Ames Laboratory and Physics Department, Iowa State University, Ames, Iowa 50011

K. A. Moler

Department of Applied Physics, Stanford University, Stanford, California 94305

(Received 10 August 1998)

We present the solution to London's equations for the magnetic fields of a vortex oriented parallel to the planes, and normal to a crystal face, of a layered superconductor. These expressions account for flux spreading at the superconducting surface, which can change the apparent size of the vortex along the planes by as much as 30%. We compare these expressions with experimental results. [S0163-1829(99)10405-3]

I. INTRODUCTION

Recently, scanning superconducting quantum interference device (SQUID) microscope magnetic imaging of interlayer vortices trapped between the planes of layered superconductors has been used to make direct measurements of the interlayer penetration depth in several layered superconductors.[1–4] These experiments provide local measurements of the interlayer supercurrent density, which have implications for the validity of the interlayer tunneling model[5] as a candidate mechanism for superconductivity in the high critical temperature cuprate superconductors.

To date the quantitative modeling of these experiments has assumed that the vortex fields at the superconductor-vacuum interface are the same as those in the bulk, neglecting the well-known effect that the magnetic fields from vortices spread as they approach the superconductor-vacuum surface from within the superconductor. Exact theoretical expressions exist for a vortex in an isotropic London's model.[6] For a vortex oriented perpendicular to the surface in a superconductor with an isotropic penetration depth λ, the fields above the surface can be approximated by a magnetic monopole located a distance λ below the surface.[6,7] This means that the spatial extent of the magnetic fields at the surface is larger than in the bulk of the superconductor. If the bulk expressions were used to fit data at the surface, the fitted value of the penetration depth would be longer than the real value. This effect must be accounted for in making quantitative estimates of the penetration depths by magnetic imaging measurements. For this purpose it is useful to examine vortex spreading at the surface for a highly anisotropic superconductor, since recent experiments have studied vortices in superconductors with $\lambda_c/\lambda_{ab} \sim 10$–$100$.

It is well known that the anisotropic London model is appropriate for describing a stack of Josephson coupled superconducting layers at length scales large compared to the interlayer spacing. In this paper we present an exact solution of London's equations for a straight vortex approaching a superconductor-vacuum interface normal to the interface, in an anisotropic superconductor. We show how flux spreading near this interface effects the magnetic fields above the interface, and show that there is good agreement between these theoretical results and scanning SQUID microscope measurements on single crystals of the layered high-T_c cuprate superconductor $Tl_2Ba_2CuO_{6+\delta}$ (Tl-2201).[1]

II. THE MODEL

A method for finding the field distribution of a straight vortex crossing a plane surface of an anisotropic superconductor has been developed in Ref. 8. We will outline this method and apply it to the case of a vortex, oriented along b in the ab plane of a uniaxial material, which crosses the plane face ca of the crystal. For a vortex not too close to the crystal corners, the crystal surface ca can be taken as an infinite plane. We choose the coordinates x,y,z corresponding to c,a,b of the crystal as shown in Fig. 1. Then the mass tensor is diagonal: $m_{xx}=m_3, m_{yy}=m_{zz}=m_1$. The standard normalization $m_1^2 m_3 = 1$ is implied. The method consists of solving London's equations for the field inside the superconductor and matching the result to a solution of Maxwell's equations in the vacuum outside the sample. For the isotropic case, the problem is simplified by the cylindrical symmetry
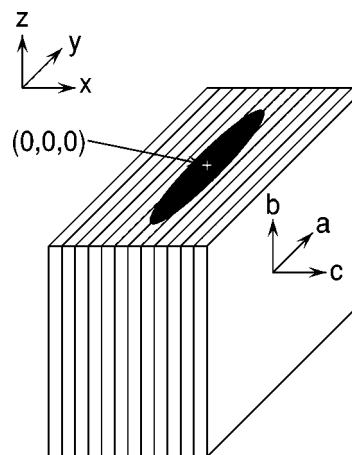

FIG. 1. Geometry and axes used in this paper. A single vortex, centered at $x=0, y=0$, emerges normally to the ac face of the crystal located at $z=0$.

of the field distribution.[6,9] This is not the case for anisotropic materials, and a more general approach is needed.

Inside the superconductor, the field $\mathbf{h}(\mathbf{r},z)$, with $\mathbf{r} = \{x,y\}$, satisfies the London equations:[10]

$$h_i - \frac{4\pi}{c}\lambda^2 m_{kl} e_{ils}\frac{\partial j_k}{\partial x_s} = \phi_0 \delta(\mathbf{r})\delta_{iz}. \tag{1}$$

Here, $\mathbf{j}$ is the current density, $\phi_0 = hc/2e$ is the superconducting flux quantum, and the average penetration depth $\lambda = (\lambda_{ab}^2 \lambda_c)^{1/3}$ $(\lambda_{ab}^2 = m_1\lambda^2, \lambda_c^2 = m_3\lambda^2)$.

Deep inside the superconductor, the field $\mathbf{h}(\mathbf{r})$ has only a z component. However, near the exit from the sample at $z = 0$, the vortex "opens up" and h_x, h_y are no longer zero. In other words, Eq. (1) is a system of three linear differential equations for h_x, h_y, and h_z with a nonzero right-hand side (RHS). The general solution is then

$$\mathbf{h} = \mathbf{h}^{(0)} + \mathbf{h}^{(v)}, \tag{2}$$

where $\mathbf{h}^{(0)}$ solves the homogeneous system with zero RHS, whereas $\mathbf{h}^{(v)}$ is a particular solution of the full system (1). The latter can be taken as the field of an infinitely long unperturbed vortex along z; this assures correct singular behavior at the vortex axis. The Fourier transform of this field is

$$\mathbf{h}^{(v)} = \frac{\phi_0}{1 + \lambda_{ab}^2 k_x^2 + \lambda_c^2 k_y^2}\hat{\mathbf{z}}. \tag{3}$$

With this choice of $\mathbf{h}^{(v)}$, the field $\mathbf{h}^{(0)}$ is the correction due to the surface of the unperturbed vortex field $\mathbf{h}^{(v)}$. We note that the Clem-Coffey result for a vortex parallel to the layers of a Josephson coupled layered superconductor reduces to $\mathbf{h}^{(v)}$ if one disregards the core correction.[11]

Because the only sample boundary is parallel to the plane xy, we Fourier transform Eq. (1) with respect to x,y. We are then left with the system of equations for $\mathbf{h}(\mathbf{k},z) = \int d\mathbf{r}\exp(-i\mathbf{k}\cdot\mathbf{r})\mathbf{h}(\mathbf{r},z)$:

$$m_1 h_x'' - (1 + m_1 k_y^2)h_x + m_1 k_x k_y h_y - i m_1 k_x h_z' = 0,$$

$$m_1 k_x k_y h_x + m_3 h_y'' - (1 + m_1 k_x^2)h_y - i m_3 k_y h_z' = 0, \tag{4}$$

$$i m_1 k_x h_x' + i m_3 k_y h_y' + (1 + m_1 k_x^2 + m_3 k_y^2)h_z = \phi_0.$$

For brevity, we have set the average λ as the unit of length so that $\lambda_{ab}^2 = \lambda^2 m_1$ and $\lambda_c^2 = \lambda^2 m_3$ are replaced with m_1 and m_3; the prime in the above equations denotes d/dz. The field $\mathbf{h}^{(0)}(\mathbf{k},z)$ satisfies the *homogeneous* system of *linear second-order ordinary differential* (with respect to the variable z) equations, i.e., it is a linear combination of exponential functions of z:

$$\mathbf{h}^{(0)}(\mathbf{k},z) = \sum_n \mathbf{H}^{(n)} e^{\alpha_n z}. \tag{5}$$

The z independent coefficients $\mathbf{H}^{(n)}(\mathbf{k})$ and $\alpha_n(\mathbf{k})$ are still to be determined. Each term in the sum (5) should satisfy separately the system (4) with zero RHS. Omitting the label n we write this system as

$$\Delta_{ij} H_j = 0 \tag{6}$$

with a symmetric matrix Δ_{ij}:

$$\Delta_{xx} = 1 + m_1 k_y^2 - m_1 \alpha^2,$$

$$\Delta_{xy} = -m_1 k_x k_y,$$

$$\Delta_{xz} = i\, m_1 k_x \alpha, \tag{7}$$

$$\Delta_{yy} = 1 + m_1 k_x^2 - m_3 \alpha^2,$$

$$\Delta_{yz} = i\, m_3 k_y \alpha,$$

$$\Delta_{zz} = 1 + m_1 k_x^2 + m_3 k_y^2.$$

The determinant of this matrix must be zero, which provides all possible values of α:

$$\alpha_{1,2} = \pm\left(\frac{1 + m_1 k^2}{m_1}\right)^{1/2}, \tag{8}$$

$$\alpha_{3,4} = \pm\left(\frac{1 + m_1 k_x^2 + m_3 k_y^2}{m_3}\right)^{1/2}. \tag{9}$$

Deep inside the superconductor, the surface correction $\mathbf{h}^{(0)}(z \to -\infty)$ must vanish, implying α_1 and α_3 must be positive. The homogeneous system (6) allows one to express (for each of these α's) two out of three components H_i in terms of the third. We obtain after simple algebra:

$$H_x^{(1)} = i\frac{1 + m_1 k_x^2}{m_1 k_x \alpha_1}H_z^{(1)}, \quad H_y^{(1)} = i\frac{k_y}{\alpha_1}H_z^{(1)}; \tag{10}$$

$$H_x^{(3)} = 0, \quad H_y^{(3)} = i\frac{\alpha_3}{k_y}H_z(3). \tag{11}$$

Thus, the field inside the sample will be determined completely after $H_z^{(1)}$ and $H_z^{(3)}$ are found from the boundary conditions at the sample surface.

The field outside the sample is described by $\operatorname{div}\mathbf{h} = 0$ and $\operatorname{curl}\mathbf{h} = 0$, so that one looks for $\mathbf{h} = \nabla\varphi$ with $\nabla^2\varphi = 0$. The general solution of Laplace's equation which vanishes at $z \to \infty$ is

$$\varphi(\mathbf{r},z) = \int \frac{d^2\mathbf{k}}{(2\pi)^2}\varphi(\mathbf{k})\,e^{i\mathbf{k}\cdot\mathbf{r} - kz}. \tag{12}$$

The two-dimensional (2D) Fourier transform is defined by

$$\varphi(\mathbf{k}) = e^{kz}\int d^2\mathbf{r}\,\varphi(\mathbf{r},z)\,e^{-i\mathbf{k}\cdot\mathbf{r}}. \tag{13}$$

The boundary conditions at the free surface $z = 0$ consist of continuity of the three field components:

$$ik_x\,\varphi = H_x^{(1)} + H_x^{(3)},$$

$$ik_y\,\varphi = H_y^{(1)} + H_y^{(3)}, \tag{14}$$

$$-k\,\varphi = h_z^{(v)} + H_z^{(1)} + H_z^{(3)}.$$

The components $H_{x,y}^{(1,3)}$ are expressed in terms of $H_z^{(1,3)}$ in Eqs. (10) and (11), so that the system (14) can be solved to

find φ along with all H_i's. We are interested here primarily in the field outside the sample:

$$\varphi(\mathbf{k}) = -\frac{\phi_0(1+m_1k_x^2)}{m_3\alpha_3[m_1k_x^2\alpha_3(k+\alpha_1)+k\alpha_3+k_y^2]}. \quad (15)$$

It is readily verified that for the isotropic material Eq. (15) reduces to the known result by Pearl: $\varphi = -\phi_0/\alpha_{is}k(k+\alpha_{is})$ where α_{is} is the isotropic version of either α_1 or α_3.[6]

Since *outside* the sample $\mathbf{h}=\nabla\varphi$, we have

$$h_{x,y}(\mathbf{k})=ik_{x,y}\varphi(\mathbf{k}), \quad h_z(\mathbf{k})=-k\varphi(\mathbf{k}). \quad (16)$$

Then, for example, the

$$h_z(\mathbf{r},z)=-\int\frac{d^2\mathbf{k}}{(2\pi)^2}k\varphi(\mathbf{k})e^{i\mathbf{k}\cdot\mathbf{r}-kz}. \quad (17)$$

In particular, the total magnetic flux through any plane $z=z_0$ is given by $h_z(k=0,z_0)=\phi_0$ as expected.

The field *inside* the sample is given by Eqs. (2), (3), and (5). The coefficients $\mathbf{H}^{(1,3)}$ in

$$\mathbf{h}^{(0)}(\mathbf{k},z)=\mathbf{H}^{(1)}e^{\alpha_1 z}+\mathbf{H}^{(3)}e^{\alpha_3 z} \quad (18)$$

are obtained by solving Eqs. (14), (10), and (11):

$$\mathbf{H}^{(1)}=\varphi(\mathbf{k})\left\{ik_x,i\frac{m_1k_x^2k_y}{1+m_1k_x^2},\frac{m_1k_x^2\alpha_1}{1+m_1k_x^2}\right\}, \quad (19)$$

$$\mathbf{H}^{(3)}=\varphi(\mathbf{k})\left\{0,\frac{ik_y}{1+m_1k_x^2},\frac{k_y^2}{\alpha_3(1+m_1k_x^2)}\right\}. \quad (20)$$

Thus, for example,

$$h_x(\mathbf{r},z)=\int\frac{d^2\mathbf{k}}{(2\pi)^2}ik_x\varphi(\mathbf{k})e^{i\mathbf{k}\cdot\mathbf{r}+\alpha_1 z}. \quad (21)$$

For what follows, we will only concern ourselves with the fields outside of the superconductor. In the experiment of Ref. 1, the component h_z was probed with a SQUID pickup loop which was much larger than the penetration depth λ_{ab}. One therefore expects the instrument to measure a flux nearly equal to the pickup loop size times

$$\mathcal{H}_z(x,y)=\int_{-\infty}^{\infty}h_z(x,y,z)\,dx. \quad (22)$$

The vortex spreads as it approaches from below the superconducting surface in the x direction as well as in the y direction; nevertheless numerical estimates show that under typical conditions the experimental signal is well represented by Eq. (22). Then we obtain:

$$\frac{\mathcal{H}_z(y,z)}{\phi_0}=\int_{-\infty}^{\infty}\frac{dk_y}{2\pi}\frac{e^{ik_yy-|k_y|z}}{m_3\alpha(\alpha+|k_y|)} \quad (23)$$

with $\alpha=\alpha_3(k_x=0)=(m_3^{-1}+k_y^2)^{1/2}$. In conventional units,

$$\frac{\mathcal{H}_z(y,z)}{\phi_0}=\int_{-\infty}^{\infty}\frac{dk_y}{2\pi}\frac{e^{ik_yy-|k_y|z}}{\alpha(\alpha+\lambda_c|k_y|)} \quad (24)$$

with $\alpha=(1+\lambda_c^2k_y^2)^{1/2}$. It is worth noting that the quantity $\mathcal{H}_z(y,z)$ depends only on λ_c.

After the substitution $\lambda_c k_y=\sinh u$, Eq. (24) takes the form

$$\pi\lambda_c\frac{\mathcal{H}_z(x,y)}{\phi_0}=\int_0^{\infty}du\,e^{-u-z'\sinh u}\cos(y'\sinh u)$$

$$=\mathrm{Re}\int_0^{\infty}du\,e^{-u-w\sinh u}$$

$$=\mathrm{Re}\left[\frac{1}{w}+\frac{\pi}{2}(\mathbf{E}_1(w)+Y_1(w))\right]. \quad (25)$$

Here, $y'=y/\lambda_c$, $z'=z/\lambda_c$, and $w=(z+iy)/\lambda_c$; $\mathbf{E}_1$ and Y_1 are Weber's and Neumann functions, see Ref. 12.

For $|w|\ll 1$ (both y and z are small relative to λ_c) we have:[12]

$$\pi\lambda_c\frac{\mathcal{H}_z(y,z)}{\phi_0}=\mathrm{Re}\left[1+\frac{w}{2}\left(\ln\frac{w}{2}+\gamma-\frac{1}{2}\right)\right]$$

$$=1+\frac{z}{2\lambda_c}\left(\ln\frac{\sqrt{y^2+z^2}}{2\lambda_c}+0.077\right)$$

$$-\frac{y}{2\lambda_c}\tan^{-1}\frac{y}{z} \quad (26)$$

($\gamma=0.577$ is Euler's constant). If $|w|\gg 1$ (at least one of y or z is large relative to λ_c), we obtain:

$$\pi\lambda_c\frac{\mathcal{H}_z(y,z)}{\phi_0}=\mathrm{Re}\left[\frac{1}{w}-\frac{1}{w^2}+O(|w|^{-4})\right]$$

$$=\frac{z\lambda_c}{y^2+z^2}-\frac{(z^2-y^2)\lambda_c^2}{(z^2+y^2)^2}+\cdots. \quad (27)$$

At large distances from the vortex exit, the second term can be neglected and λ_c drops out of the result; this is expected since the field there is approaching the Coulomb form with no trace of material properties.

To form a complete picture of the field distribution outside the sample, we imagine that the same SQUID probe is oriented in the xz plane so that the y component of the field (integrated over the probe area) is measured. Then the SQUID flux will be nearly equal to the pickup loop size times

$$\mathcal{H}_y(y,z)=\int_{-\infty}^{\infty}h_y(x,y,z)\,dx=\int_{-\infty}^{\infty}\frac{dk_y}{2\pi}ik_y\varphi(0,k_y)e^{ik_yy-k_yz}. \quad (28)$$

The two-dimensional field $\vec{\mathcal{H}}$ satisfies $\mathrm{div}\vec{\mathcal{H}}=\mathrm{curl}\vec{\mathcal{H}}=0$. Hence, it can be written as $\vec{\mathcal{H}}=\nabla\Phi$ with $\nabla^2\Phi=0$. This implies that $\mathcal{H}_z$ and $\mathcal{H}_y$ are real and imaginary parts of the same analytic function given in Eq. (25):[13]

$$\mathcal{H}_y(y,z)=\frac{\phi_0}{\pi\lambda_c}\mathrm{Im}\left(\frac{1}{w}+\frac{\pi}{2}[\mathbf{E}_1(w)+Y_1(w)]\right). \quad (29)$$

In particular, the asymptotic form of this function for $w\gg 1$ can be written as
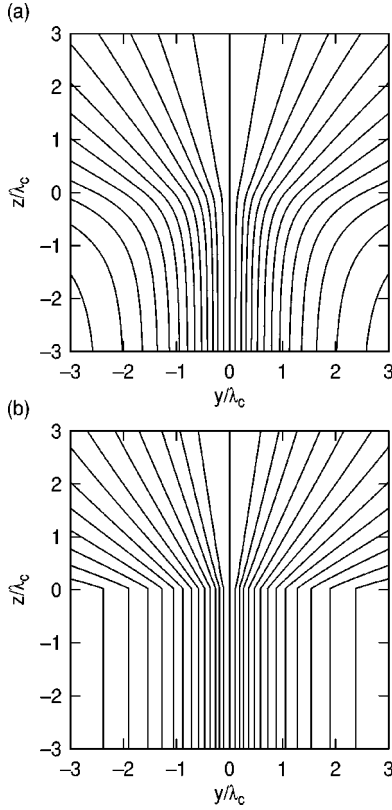
FIG. 2. Streamline mapping of $\vec{\mathcal{H}}(y,z)$, the magnetic field integrated over x, for a single interlayer vortex shown in Fig. 1. The spacing of the streamlines is proportional to $(\partial\mathcal{H}_z/\partial y)^{-1}$ at $z=-3\lambda_c$. (a) is the present model, which includes vortex spreading; (b) is for a model which neglects field spreading below the surface.

$$\frac{1}{w} - \frac{1}{w^2} \approx \frac{1}{w+1}, \tag{30}$$

which implies that at large distances the field $\vec{\mathcal{H}}$ behaves as a field of a 2D "charge" situated at $z=-\lambda_c$.

III. RESULTS

Figure 2(a) shows streamlines of $\vec{\mathcal{H}}(y,z)$ for a single anisotropic vortex centered at $x=0, y=0$. These streamlines were generated numerically as follows: the starting points of the lines were at $z/\lambda_c=-3$, with a spacing in y between the lines proportional to $(\partial\mathcal{H}_z/\partial y)^{-1}$ at $z/\lambda_c=-3$. Small steps $z=z+\Delta z, y=y+\Delta y$, with $\Delta z=\delta\sin\theta, \Delta y=\delta\cos\theta$, were generated, with $\theta=\tan^{-1}(\mathcal{H}_z(y,z)/\mathcal{H}_y(y,z))$. The fields were recalculated at the new positions, and then the process was repeated until $|z/\lambda_c|>3$ or $|y/\lambda_c|>3$. Figure 2(b) shows the results if field spreading below the surface is neglected:

$$b_z(x,y,z<0) = \frac{\phi_0}{2\pi\lambda_{ab}\lambda_c} K_0(\tilde{R}), \tag{31}$$

where K_0 is a modified Bessel function of the second kind of order 0, $\tilde{R}=[(s/2\lambda_{ab})^2+(x/\lambda_{ab})^2+(y/\lambda_c)^2]^{1/2}$, and s is the interplanar spacing.[11] For $s\ll\lambda_{ab}$, Eq. (31) has the Fourier transform given in Eq. (3). The fields for $z>0$ are given by
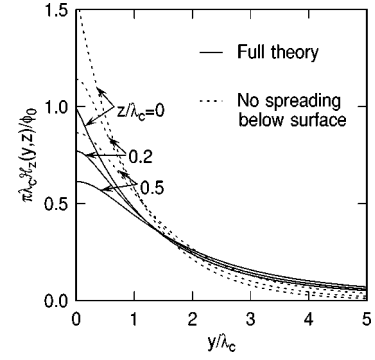

FIG. 3. Plot of $\mathcal{H}_z(y,z)$ for a single interlayer vortex normal to the superconducting surface $z=0$, as a function of y/λ_c, for fixed z values, where y is the distance from the center of the vortex along a plane direction, and λ_c is the interlayer penetration depth.

$$b_z(\mathbf{r},z) = \int \frac{d^2\mathbf{k}}{(2\pi)^2} b_z(\mathbf{k}) e^{i\mathbf{k}\cdot\mathbf{r}-kz}, \tag{32}$$

where

$$b_z(\mathbf{k}) = \int d^2\mathbf{k} b_z(x,y,z=0)e^{-i\mathbf{k}\cdot\mathbf{r}} \tag{33}$$

(Ref. 14). The fields in the x and y directions are treated similarly, using the relations $b_x(\mathbf{k})=-ik_x b_z(\mathbf{k})/k$, and $b_y(\mathbf{k})=-ik_y b_z(\mathbf{k})/k$. The calculated fields were integrated over x and streamlines were generated just as for the exact London expressions. This is the procedure used to model the experimental results in Ref. 1. In both cases the fields extend into the vacuum nearly isotropically at large distances, as if a point monopole source were placed near $z=-\lambda_c$. In the full treatment, Fig. 2(a), the fields spread as the vortex approaches the surface from inside the superconductor.

A one-dimensional rendering of our results above the surface of the superconductor is shown in Fig. 3, which plots $\pi\lambda_c\mathcal{H}_z(y,z)/\phi_0$ as a function of y/λ_c for several values of z/λ_c. For comparison, the results neglecting vortex spreading are also shown. Note that $\mathcal{H}_z(0,0)$, which approximately indicates the peak signal in an experiment, is overestimated by a factor of $\pi/2$ if vortex spreading is neglected. Also, the full width at half maximum (FWHM) of the flux contour is $1.87\lambda_c$ for the full theory, while it is $1.37\lambda_c$ if flux spreading is neglected. Therefore the neglect of flux spreading could result in an overestimate of λ_c by 30%.

IV. COMPARISON WITH EXPERIMENT

Previous analyses of experimental data,[1,2] neglected the effect of vortex spreading at the surface. In retrospect, this neglect was not unreasonable, given the quantitative agreement between the interlayer coupling strength obtained from vortex imaging measurements and from the Josephson plasma resonance.[2] With the full theory presented in this paper, it is now possible to quantitatively examine this assumption. However, we note that there are additional systematic experimental uncertainties in this technique. These errors include the effect of macroscopic screening currents which may create a slightly inhomogeneous background, a relative angle of 10–20 degrees between the surface of the
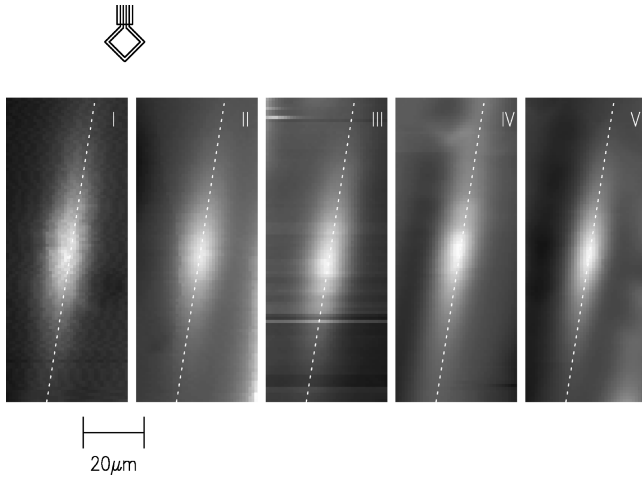
FIG. 4. Grey-scale images of five interlayer vortices in the high-T_c cuprate superconductor Tl-2201. The scaling corresponds to $0.11\phi_0$(I), $0.16\phi_0$(II), $0.13\phi_0$(III), $0.22\phi_0$(IV), and $0.19\phi_0$(V) full-scale variation from black to white in the integrated flux through the pickup loop.
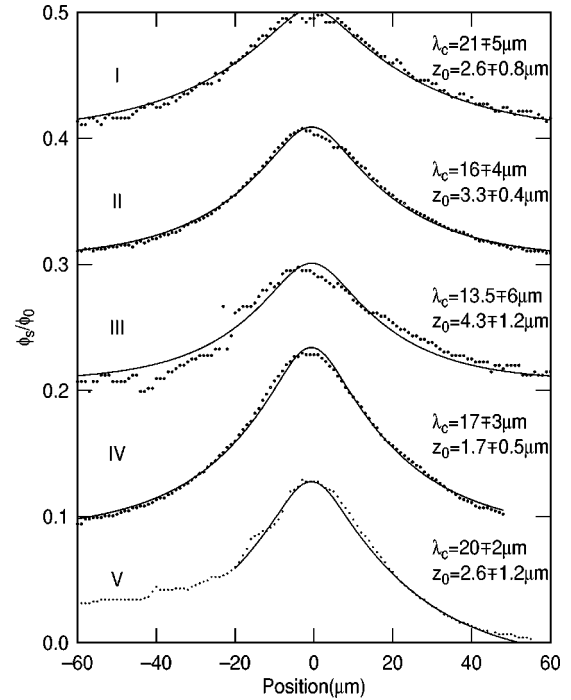

FIG. 5. Cross sections along the plane directions through the images of Fig. 4. Each successive curve is offset by 0.1 unit for clarity. The dots are the data; the lines are fits to the present model as described in the text.

superconductor and the SQUID pickup loop, the uncertainty in the exact value of the height of the pickup loop, and some effect of the leads to the pickup loop on the effective shape of the pickup loop. We estimate that these errors may also be as large as 30%.

Figure 4 shows gray-scale images of five interlayer vortices in Tl-2201 magnetically imaged using a scanning SQUID microscope.[1] In these experiments the experimental signal is equal to the integrated magnetic flux through the pickup loop. The vortices appear elliptical in shape, with the long axis (parallel to the planes) nearly vertical in these images. The spatial extent of the vortex images perpendicular to the planes is limited simply by the size of the pickup loop. The spatial extent parallel to the planes is set primarily by the interplanar penetration depth. Figure 5 shows cross sections through the experimental data along the direction parallel to the planes as indicated by the dashed lines in Fig. 4.

To generate a theoretical expression for fitting the experiment results, we use the full expression [Eq. (15)] for the magnetic fields, taking the a-axis penetration depth equal to 0.17 μm.[15] An evaluation of Eq. (15) gives the z component of the field at a given height z_0 above the sample surface. This field is then numerically integrated over the shape of the pickup loop to obtain the total theoretical flux $\Phi_s(x,y,z)$ through the pickup loop as a function of the pickup loop position and the c-axis penetration depth λ_c. In this case the pickup loop used was a square 8.2 μm on a side, with a 1 μm linewidth, and a superconducting shield 5 μm wide which extends to the top corner of the pickup loop, as indicated by the inset of Fig. 4. For our modeling we add to the flux through the pickup loop one third of the flux intercepting an area 5 μm by 5 μm on a side, starting at the upper corner of the pickup loop, to account for flux focusing effects from the superconducting shield. The solid lines in Fig. 5 are best fits of the cross section $\Phi_s(x=0,y,z=z_0)$ to the experimental data, using the interlayer penetration λ_c, the height of the pickup loop z_0, and an offset flux, representing a

small uncertainty of the background signal, as free parameters. The best fit values for each vortex are displayed in the figure, with uncertainties assigned using a doubling of the χ^2 value as a criterion. Reasonable agreement is obtained between experimental and theoretical cross sections. The average value for λ_c, using a weighting inversely proportional to the square of the uncertainties, is $\lambda_c = 18.3 \pm 3$ μm.

For comparison, a similar analysis of the same vortices neglecting the effect of vortex spreading resulted in a weighted average best-fit value of $\lambda_c = 19 \pm 2$ μm. This comparison is surprising at first, since the theoretical FWHM at the surface is reduced by 30% when the vortex spreading is neglected. However, the uncertain value of the height of the pickup loop compensates for the assumption of negligible vortex spreading below the surface. When the spreading below the surface is neglected, the fitting routine compensates by picking a higher value of z_0, thereby moving the spreading to the vacuum rather than the superconductor.

In conclusion, we have presented a solution to London's equation for the case of an interlayer vortex approaching a superconducting surface normal to the surface and parallel to the planes. This model is appropriate for experiments which magnetically image interlayer vortices. Good agreement with available experiments is obtained with this model, allowing the quantitative determination of the interlayer penetration depths from these measurements.

[1] K. A. Moler, J. R. Kirtley, D. G. Hinks, T. W. Li, and Ming Xu, Science **279**, 1193 (1998).

[2] A. A. Tsvetkov, D. van der Marel, K. A. Moler, J. R. Kirtley, J. L. de Boer, A. Meetsma, Z. F. Ren, N. Koleshnikov, D. Dulic, A. Damascelli, M. Grüninger, J. Schützmann, J. W. van der Eb, H. S. Somal, and J. H. Wang, Nature (London) **395**, 360 (1998).

[3] J. R. Kirtley, K. A. Moler, G. Villard, and A. Maignan, Phys. Rev. Lett. 81, 2140 (1998).

[4] J. R. Kirtley, K. A. Moler, J. A. Schlueter, and J. M. Williams, J. Phys. Condens. Matter (to be published).

[5] J. Wheatley, T. Hsu, and P. W. Anderson, Nature (London) **333**, 121 (1988); P. W. Anderson, Physica C **185**, 11 (1991); Phys. Rev. Lett. **67**, 660 (1991); Science **256**, 1526 (1992); S. Chakravarty, A. Sudbø, P. W. Anderson, and S. Strong, *ibid.* **261**, 331 (1993).

[6] J. Pearl, J. Appl. Phys. **37**, 4139 (1966).

[7] A. M. Chang, H. D. Hallen, L. Harriott, H. F. Hess, H. L. Kao, J. Kwo, R. E. Miller, R. Wolfe, and J. van der Ziel, Appl. Phys. Lett. **62**, 1974 (1992).

[8] V. G. Kogan, A. Yu. Simonov, and M. Ledvij, Phys. Rev. B **48**, 392 (1993).

[9] J. R. Clem, Phys. Rev. B **1**, 2140 (1970).

[10] V. G. Kogan, Phys. Rev. B **24**, 1572 (1981).

[11] J. R. Clem and M. W. Coffey, Phys. Rev. B **42**, 6209 (1990).

[12] I. S. Gradshtein and I. M. Ryzhik, *Tables of Integrals, Series and Products* (Academic Press, New York, 1965).

[13] L. D. Landau and E. M. Lifshitz, *Electrodynamics of Continuous Media* (Pergamon, New York, 1984).

[14] Bradley J. Roth, Nestor G. Sepulveda, and John P. Wikswo, J. Appl. Phys. **65**, 361 (1988).

[15] F. Zuo, D. Vacaru, H. M. Duan, and A. M. Hermann, Phys. Rev. B **47**, 8327 (1993).